Improved Cleaning of Hydrophilic Protein-Coated Surfaces using the Combination of Nanobubbles and SDS

Guangming Liu and Vincent S. J. Craig*

Department of Applied Mathematics, Research School of Physical Sciences and Engineering, The Australian National University, Canberra, ACT 0200, Australia

ABSTRACT The use of nanobubbles, the common surfactant sodium dodecyl sulfate (SDS), and nanobubbles in combination with SDS as cleaning agents to remove lysozyme from the solid−liquid interface has been investigated using a quartz crystal microbalance on both hydrophobic and hydrophilic surfaces. On the hydrophobic surface, significant amounts of protein remained on the surface after 10 cycles of nanobubble treatment for 10 s periods in phosphate buffer. The cleaning efficiency of SDS was far superior and was shown to remove approximately 90% of the protein. The use of nanobubbles in combination with SDS failed to improve the cleaning efficiency further. On the other hand, lysozyme on the hydrophilic surface cannot be removed effectively by either 10 cycles of cleaning with nanobubbles or 10 cycles of cleaning with SDS. Nevertheless, the protein can be removed completely after 6 cycles of cleaning with nanobubbles in combination with SDS.

KEYWORDS: Nanobubbles • quartz crystal microbalance (QCM) • lysozyme • sodium dodecyl sulfate (SDS) • cleaning • electrolysis • degassing

INTRODUCTION

The relatively recent discovery of very small gas entities at the solid−liquid interface known as nanobubbles has led to much effort aimed at understanding the physical properties of such small bubbles (1−23) and much more recently, efforts at revealing potential applications of nanobubbles, such as antifouling treatments (24, 25). Theoretically, such small bubbles should dissolve and disappear rapidly because of the high Laplace pressure inside the bubbles (1, 2). However, recent publications suggested that nanobubbles are indeed stable and that this stability is related to a lower than expected interfacial curvature (10). Some experiments have supported the existence of nanobubbles at the hydrophobic surface, but found no support for their existence on the hydrophilic surface (7, 8). In contrast, other experiments revealed that nanobubbles can be formed on both hydrophobic and hydrophilic surfaces (6, 12, 15, 24). Generally, the formation of nanobubbles on the hydrophobic surface is much easier than the hydrophilic surface, and the nanobubbles will be more stable on the hydrophobic surface (3, 10). It is believed that surface supersaturation of gas is a prerequisite for generating nanobubbles at the solid−liquid interface (10). Several techniques including solvent exchange (10), temperature change (12), and electrolysis (13) have been employed to produce nanobubbles at the solid−liquid interface. The former two methods can be employed in conjunction with any surface (usually hydrophobic), whereas the last method requires a conducting surface but has the advantage of a greater level of control over nanobubble production and is more suitably employed on hydrophilic surfaces.

Previous papers have demonstrated that electrochemically generated nanobubbles facilitate the removal of bovine serum albumin (BSA) from both hydrophobic and hydrophilic surfaces using atomic force microscopy (AFM) (26) and the quartz crystal microbalance (QCM) technique (27). It was shown that with a few cycles of treatment the protein can be completely removed and the cleaning efficiency of a 10 s nanobubble treatment is analogous to a 20 min treatment with sodium dodecyl sulfate (SDS) (27). In practice, the amount of protein adsorbed and the adsorption strength will vary widely for different proteins because of different protein-surface interactions (28). Thus, for some strongly adsorbed proteins, it is evident that significant amounts of protein will remain on the surface even after extensive cleaning (29). Here, we have chosen to use the protein lysozyme which adsorbs more strongly on both hydrophobic and hydrophilic surfaces than BSA and therefore provides a strong cleaning challenge. We have investigated how the cleaning efficiency can be improved by using surfactant and nanobubbles as cleaning agents in combination.

EXPERIMENTAL SECTION

The study of nanobubbles is in its infancy. There is currently no method that can reliably produce data on the efficiency of nanobubble production. The available evidence is that it is a stochastic process dependent upon the surface chemistry, surface roughness, and method of inducing nanobubble production. To get reliable statistics, the production of a large number of nanobubbles needs to be followed. In this sense, QCM is suitable as the production of nanobubbles over the whole surface contributes to the change in resonance frequency

* To whom correspondence should be addressed. E-mail: vince.craig@anu.edu.au.
Received for review October 29, 2008 and accepted December 28, 2008

DOI: 10.1021/am800150p

measured, but it is not currently possible to determine the nanobubble size and areal density from the frequency response, as we expect that the frequency response is not strictly proportional to the volume of nanobubbles produced if the size of nanobubbles is not held constant. AFM is currently the best method for measuring the size of nanobubbles but it is not suitable for measuring the production of nanobubbles over areas that are statistically significant and it cannot yield quantitative data on adsorption. For this reason, we have used QCM and adopted a standard procedure for the production of nanobubbles in these measurements.

A KSV (Helsinki, Finland) Quartz Crystal Microbalance employing a 5 MHz AT cut quartz crystal with gold electrodes (rms roughness ≈ 3 nm) was used to follow the adsorption and desorption of proteins and surfactants as well as the production and removal of nanobubbles. After RF plasma treatment at a power level of 30 W for 60 s, the gold surface of the quartz crystal was exposed to a 5 mM ethanolic solution of 1-dodecanethiol (AR grade, Aldrich) for a period of 12 h when a hydrophobic surface was desired. When a hydrophilic surface was required the gold electrode surface of the quartz crystal was exposed to a 5 mM ethanolic solution of 11-mercaptoundecanoic acid (AR grade, Aldrich) for a period of 12 h following the same RF plasma treatment as above. Following treatment, the crystal was thoroughly rinsed in ultrapure ethanol and dried under a nitrogen stream. The monolayers were characterized by measurement of the contact angle obtained with pure water using a KSV Cam 200 Contact Angle Goniometer. After modifying the resonator surfaces, the advancing contact angle (Θ_A) was ~102° and the receding contact angle (Θ_R) was ~95° for the hydrophobic surface. For the hydrophilic surface, Θ_A and Θ_R were 59 and 39°, respectively. Modifications were also made to the QCM permitting electrolysis to be performed using the gold surface of the quartz crystal as the working electrode, without any change to the mounting of the crystal. This is important as disturbance of the crystal can lead to significant changes in the measured resonance frequency.

Electrochemical treatment was achieved using the gold coated quartz resonator as the cathode and a stainless steel surface as the anode. When a DC voltage (~3.2 V) was applied between the resonator and the stainless steel surface, water was electrolyzed into molecular hydrogen and oxygen and the supersaturated hydrogen formed nanobubbles at the liquid−resonator interface. Typically, the time allowed for electrolysis was 10 s for each cycle.

QCM is commonly employed to follow the adsorption of surfactants, particles, polymers and proteins to a substrate (30−35). The change in resonance frequency (Δf) of the crystal can be related to the adsorbed amount (Δm) using the Sauerbrey equation (36), which is known to perform well for films that behave elastically.

$$\Delta m = -\frac{\rho_q l_q}{f_0}\frac{\Delta f}{n} = -C_{QCM}\frac{\Delta f}{n} \quad (1)$$

Where f_0 is the fundamental frequency, n is the overtone number, ρ_q and l_q are the specific density and thickness of the quartz crystal, respectively. C_{QCM} (= 0.177 mg m^{-2} Hz^{-1} for our crystals) is the mass sensitivity constant. In the case of adsorbed proteins, the mass calculated using the Sauerbrey equation, hereafter called the Sauerbrey mass, also includes a contribution due to the mass of entrained water in the film and therefore adsorbed amounts determined by QCM routinely exceed adsorbed amounts determined by other methods. The degree of solvent coupling can be determined by use of deuterated solvents (37), or comparison with other methods. The resonance frequency is also strongly influenced by the density and viscosity of the solvent in which the crystal is immersed as described by the equation of Kanazawa and Gordon (38).

$$\Delta f = -n^{0.5} f_0^{1.5} (\eta_l \rho_l / \pi \mu_q \rho_q)^{0.5} \quad (2)$$

Where n is the overtone number, μ_q is the shear modulus of quartz, ρ_q is the density of quartz, and ρ_l and η_l are the density and viscosity of the liquid medium, respectively. For this reason, protein adsorption studies are routinely conducted such that a baseline resonance frequency value is first obtained in the same solvent without protein. Thus upon exposure to the protein solution the reduction in resonance frequency is related only to the protein adsorption and is described by the Sauerbrey equation (i.e., eq 1). The presence of nanobubbles on the surface will alter the resonance frequency, as the effective density and viscosity of the solvent in contact with the crystal is reduced. Additionally, there may be an effect due to a change in hydrodynamic boundary condition (39−41). Thus an increase in the resonance frequency is attributable to the presence of nanobubbles on the surface, though at this stage we cannot quantitatively determine the nanobubble surface density or morphology. Nonetheless, the presence and removal of nanobubbles can be semiquantitatively followed through changes in the resonance frequency. In the present study, all the results were obtained from the measurements of frequency shifts in the third overtone (n = 3) and were conducted at 25 °C. The third overtone is preferred over the fundamental overtone, as the resonator is less affected by mechanical forces associated with mounting the resonator, in comparison to the fundamental frequency.

All water used was prefiltered through a coarse wool filter, charcoal filter and reverse osmosis membrane before a final filtration through a Millipore Gradient system (Memtec) giving a resistivity of 18.2 MΩ cm^{-1}. Phosphate buffer (PB, 10 mM, pH 7.4) was prepared using potassium phosphate (KH_2PO_4) and sodium phosphate dibasic (Na_2HPO_4). When it was necessary to remove nanobubbles from the surface, the cell was rinsed with degassed phosphate buffer or degassed SDS/PB solution (SDS in phosphate buffer solution).

Degassing was achieved by exposing the solutions to vacuum (~1 torr) and mechanical disturbances for at least 2 h before rinsing the cell. Once degassed, these solutions were maintained at low pressure, except when rinsing the cell to ensure they remained degassed. Lysozyme from chicken egg white (M_w ≈ 14.7 kDa) was purchased from Fluka. Sodium dodecyl sulfate (SDS) was purchased from BDH Biochemical and purified by recrystallization from high purity ethanol prior to use.

RESULTS AND DISCUSSION

The study of nanobubbles is still somewhat within its infancy and hence the reason for the stability of nanobubbles is still not fully resolved. It is clear that for hydrophobic surfaces, the contact angle measured with the nanoscale gaseous phase (typically 165°) is far greater than that of the bulk gaseous phase (typically 110°) and as a consequence the internal pressure is lower than would otherwise be expected and that this contributes to their stability (10). Further, nanobubbles have been widely observed on hydrophobic surfaces and less commonly seen on hydrophilic surfaces. For this reason, we first present and discuss data obtained using a hydrophobic surface.

Hydrophobic Surfaces. SDS is a commonly employed surfactant in the removal of proteins. In Figure 1, we

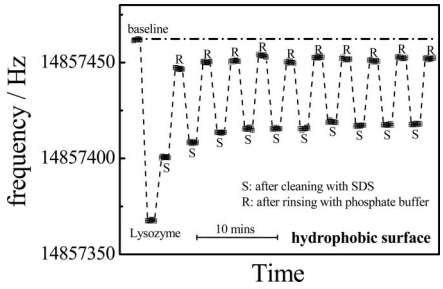

FIGURE 1. Resonance frequency observed for lysozyme on a hydrophobic surface during washing cycles using SDS as a detergent. The baseline resonance frequency is obtained for a gold coated crystal bearing a monolayer of 1-dodecanethiol in phosphate buffer. S indicates the resonance frequency measured after 20 min of cleaning with SDS and R indicates the resonance frequency measured after rinsing with phosphate buffer. Ten cycles of SDS cleaning and phosphate buffer rinses are shown. Note that the data obtained during the rinsing process are very noisy and have been removed from this and subsequent figures for clarity. The time scale is indicated by the scale bar.

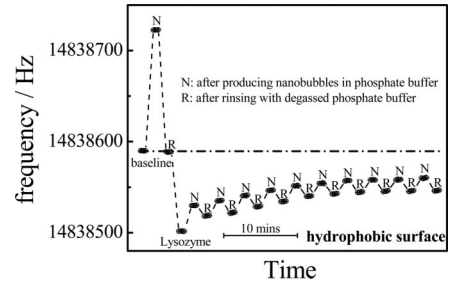

FIGURE 2. Resonance frequency observed for a series of nanobubble production and removal cycles on a hydrophobic surface in phosphate buffer. The baseline resonance frequency is obtained for a gold coated crystal bearing a monolayer of 1-dodecanethiol in phosphate buffer. Before lysozyme was introduced, nanobubbles were produced and removed, and the baseline signal was recovered. N indicates the resonance frequency measured after 10 s of electrochemical treatment to produce nanobubbles and R indicates the resonance frequency measured after the removal of such nanobubbles by rinsing with degassed phosphate buffer. Subsequently, lysozyme was introduced and the resonance frequency was measured again following a rinse with phosphate buffer. Ten further cycles of nanobubble production and removal are shown. The time scale is indicated by the scale bar.

have used SDS to remove lysozyme from a model hydrophobic surface. In QCM measurements one usually interprets the data in terms of a shift in resonance frequency from a suitable baseline. Here, we have measured the baseline frequency in phosphate buffer solution (shown as a horizontal dotted line). Upon exposure to lysozyme (1 mg mL^{-1}) and rinsing with buffer solution the resonance frequency has shifted lower by ~95 Hz, this corresponds to an adsorbed protein Sauerbrey mass of ~5.6 mg m^{-2}. Note that this exceeds the literature value (42) of 3.7 mg m^{-2} as the QCM includes an additional mass due to entrained water in the protein film. As the rinsing process introduces injection spikes into the data, this data has been removed from the figures in this paper, as has the data obtained during system equilibration for an example of the raw data please refer to our earlier work (27). The protein is then treated with SDS containing buffer solution (17 mM SDS, above CMC) and rinsed with the buffer. After rinsing with buffer solution upon exposure to SDS the frequency is seen to decrease, corresponding to the adsorption of SDS and the small changes of viscosity and density. Ten cycles are shown; however, it is clear that the cleaning takes place in the initial few cycles, which results in ~ 90% of the protein being removed. The remaining protein is clearly strongly adsorbed and resistant to removal. This suggests that some parts of the protein surface adsorb more strongly than others, reflecting the heterogeneity of the protein−surface interactions.

In Figure 2, we investigate the cleaning of lysozyme from a hydrophobic surface using nanobubbles. As above, the baseline is obtained in buffer solution. Upon application of 3.2 V for 10 s, it is evident that the production of nanobubbles on a hydrophobic surface can be readily achieved electrochemically and is revealed by the increase in resonance frequency. Upon introduction of the degassed phosphate buffer the nanobubbles were removed completely as evidenced by the return of the resonance frequency to the baseline value. Following this, the surface was exposed to lysozyme (1 mg mL^{-1}) for a period of 60 min and then the QCM cell was rinsed with phosphate buffer. The resonance frequency dropped by ~ 90 Hz. This corresponds to a Sauerbrey mass of ~5.3 mg m^{-2}, which again is greater than that reported in the literature and this again is attributed to the entrained water in the film to which the QCM signal is sensitive. The surface excess is also much larger than previously obtained for BSA adsorbed on a hydrophobic surface using QCM (~2.4 mg m^{-2}) (27), indicating that the affinity of lysozyme for the hydrophobic surface is greater than BSA. We present 10 cycles of nanobubble production and removal. It is evident that although nanobubbles are able to remove the protein from the surface, a significant amount of protein remains on the surface after 10 cycles of cleaning. It appears that the protein concentration on the surface has reached a plateau at this point and further cycles of nanobubble production are unable to remove significant amounts of protein. Clearly, the protein cannot be removed completely from the surface by using nanobubbles in phosphate buffer. Note that we have previously shown that the changes in resonance frequency observed and removal of the protein cannot be attributed to the breakdown of the hydrophobic or hydrophilic monolayer, as well as the electromagnetic field (27). Further, we also note that the frequency change due to nanobubble production initially obtained on the bare 1-dodecanethiol surface is far greater than the frequency change obtained during protein removal. This is simply due to differences in the level of gas supersaturation, as the initial production of nanobubbles took place in a buffer solution that had not been degassed, whereas subsequent electrochemical treatments all take place in degassed buffer solutions (27). Additionally, the different surface chemistries between the bare thiol surface and the lysozyme coated surface may also lead to different efficiencies of nanobubble production.

Following each treatment with nanobubbles, they are removed by the introduction of degassed phosphate buffer. By taking the resonance frequency at this stage of the cycle relative to the baseline value, we can quantify the amount of protein remaining on the surface after each cycle. Even after ten cycles of treatment approximately 50% of the

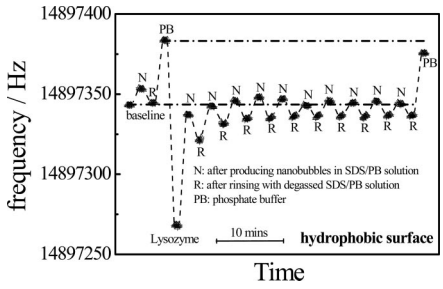

FIGURE 3. Resonance frequency observed for a series of nanobubble production and removal cycles on a hydrophobic surface in SDS/PB solution. The baseline resonance frequency is obtained for a gold coated crystal bearing a monolayer of 1-dodecanethiol in SDS/PB solution. Before lysozyme was introduced, nanobubbles were produced and removed in SDS/PB solution and the SDS/PB solution was replaced by phosphate buffer. N indicates the resonance frequency measured after 10 s of electrochemical treatment to produce nanobubbles and R indicates the resonance frequency measured after the removal of such nanobubbles by rinsing with degassed SDS/PB solution. Subsequently, lysozyme was introduced and the resonance frequency was measured again following a rinse with phosphate buffer. Ten further cycles of nanobubble production and removal in SDS/PB solution are shown. The time scale is indicated by the scale bar.

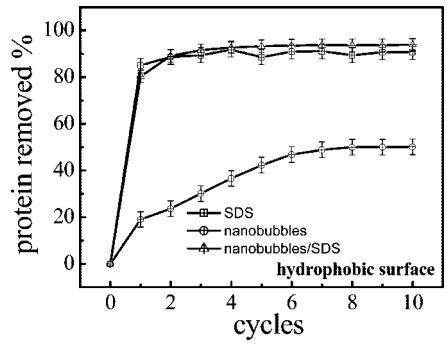

FIGURE 4. Cleaning efficiency obtained using nanobubbles, SDS, or nanobubbles/SDS on a hydrophobic surface. Each cycle is either 10 s of nanobubble production followed by nanobubble removal by means of exchanging the solvent with degassed phosphate buffer (or degassed SDS/PB solution) or 20 min exposure to 17 mM SDS in phosphate buffer followed by rinsing with phosphate buffer (without SDS). The noise level in our frequency measurement is typically less than 1 Hz; however, the main contribution to uncertainty in our measurement is instrumental drift over the time scale of our measurement, which is typically 3 Hz or less. Therefore the error bars correspond to an error of 3 Hz in our measurements.

protein remains on the surface. In this case, it is apparent that SDS is able to remove lysozyme from a hydrophobic surface more effectively than nanobubbles. However, it is likely that the cleaning mechanism is very different for SDS and nanobubbles and therefore when used in conjunction they may show synergistic effects. SDS will enhance cleaning both by adsorbing to the hydrophobic surface and to the protein, whereas nanobubbles are thought to act by a mechanical means whereby the protein is transported from the solid−liquid interface to the liquid−gas interface by the expanding three-phase line during the growth of the bubble (26). Additionally the effectiveness of nanobubbles may be expected to increase in the presence of SDS as the lysozyme/surface interaction is weakened.

To test this, we used a solution of 17 mM SDS in 10 mM phosphate buffer (SDS/PB) to replace the phosphate buffer as an electrolyte for the generation of nanobubbles. The results are shown in Figure 3. First, it is demonstrated that nanobubbles can be produced electrochemically in a SDS/PB solution on the hydrophobic surface, and the nanobubbles can be removed completely by using the degassed SDS/PB solution. Then, the SDS/PB solution was replaced by phosphate buffer. This results in an increase in frequency as the SDS is desorbed from the surface, which is subsequently exposed to a 1 mg mL^{-1} lysozyme in phosphate buffer. The QCM cell was rinsed with phosphate buffer after an ∼60 min adsorption of lysozyme. The outcome is a decrease in frequency of ∼114 Hz corresponding to a Sauerbrey mass of ∼6.7 mg m^{-2}. This is considerably higher than the observed levels of protein adsorption obtained in Figures 1 and 2. We believe that this reflects a variation in how the protein is delivered to the surface and the nonequilibrium nature of the adsorption.

Treatment with nanobubbles in the presence of SDS was then commenced. Ten cycles of nanobubble production and removal for 10 s periods are shown in this figure. It can be seen that ∼94% of the protein is removed from the surface after 10 cycles of nanobubble production and removal in SDS/PB solution (hereafter called nanobubbles/SDS), indicating that the cleaning efficiency of nanobubbles/SDS is much higher than treatment with nanobubbles alone but comparable to treatment with SDS alone. This is shown more clearly in Figure 4 where we have compared the cleaning efficiencies of nanobubbles, SDS and nanobubbles/SDS on the hydrophobic surface. First of all, the cleaning efficiency of the 20 min treatment with SDS is better than the 10 s treatment with nanobubbles. This is different from the previous result obtained with the protein BSA on a hydrophobic surface where the cleaning efficiency of SDS was analogous to the nanobubbles (27). This is understandable because the removal of protein from the surface by nanobubbles is dominated by the attachment of protein to the expanding three-phase line as the nanobubbles grow, whereas the removal of protein by SDS is affected by the complexation between protein and surfactant, which arises because of both electrostatic and hydrophobic interactions (43−45), and the adsorption of the surfactant to the substrate. In the BSA system, the protein and surfactant were both negatively charged under the buffer conditions, and therefore the electrostatic interactions should oppose complexation. However, the electrostatic interactions in the lysozyme (pI ∼11) (46) system are attractive, thereby resulting in an increase in complexation between protein and surfactant. Thus, the cleaning efficiency of SDS in relation to lysozyme is expected to be better than nanobubbles.

The cleaning efficiency of the 10 s treatment with nanobubbles/SDS is very similar to the treatment with SDS alone. Thus in this case, there is no obvious synergy in the cleaning action. Given the proposed means by which cleaning is achieved this is surprising. A possible explanation for the generally poor performance of nanobubbles as cleaning agents on the hydrophobic substrate is related to the wettability of the surface. The adsorption of protein to the surface will result in a reduction in hydrophobicity. The production of a gas phase is energetically more favorable

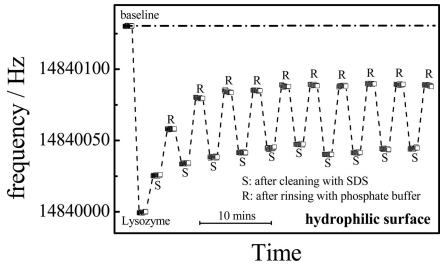

FIGURE 5. Resonance frequency observed for lysozyme on a hydrophilic surface during washing cycles using SDS as a detergent. The baseline resonance frequency is obtained for a gold coated crystal bearing a monolayer of 11-mecaptoundecanoic acid in phosphate buffer. S indicates the resonance frequency measured after 20 min of cleaning with SDS and R indicates the resonance frequency measured after rinsing with phosphate buffer. Ten cycles of SDS cleaning and phosphate buffer rinses are shown. The time scale is indicated by the scale bar.

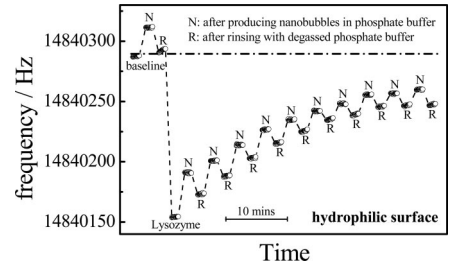

FIGURE 6. Resonance frequency observed for a series of nanobubble production and removal cycles on a hydrophilic surface in phosphate buffer. The baseline resonance frequency is obtained for a gold-coated crystal bearing a monolayer of 11-mecaptoundecanoic acid in phosphate buffer. Before lysozyme was introduced, nanobubbles were produced and removed and the baseline signal was recovered. N indicates the resonance frequency measured after 10 s of electrochemical treatment to produce nanobubbles and R indicates the resonance frequency measured after the removal of such nanobubbles by rinsing with degassed phosphate buffer. Subsequently, lysozyme was introduced and the resonance frequency was measured again following a rinse with phosphate buffer. Ten further cycles of nanobubble production and removal are shown. The time scale is indicated by the scale bar.

on a hydrophobic substrate than a hydrophilic substrate; therefore, we expect that nanobubbles preferentially form on the more hydrophobic regions of the surface. Following the first treatment cycle, the surface will have a spatially varying wettabillity, whereby the regions of the surface that have been cleaned of protein are more hydrophobic and therefore nanobubble production is favored in these already clean regions. Hence nanobubbles are produced on regions that have already been cleaned and further cycles of treatment have very little effect.

Hydrophilic Surfaces. Most practical surfaces where fouling is an issue will be relatively hydrophilic. We have also investigated the cleaning of these surfaces. In Figure 5, the lysozyme adsorption on the hydrophilic surface, results in a frequency change of approximately −131 Hz. This corresponds to a Sauerbrey mass of ∼7.7 mg m^{-2}. The greater adsorbed amount obtained on the hydrophilic surface with respect to the hydrophobic surface is attributable to differences in the interactions between lysozyme and the surfaces. The adsorption of lysozyme on the hydrophobic surface is dominated by hydrophobic interactions, whereas the adsorption of lysozyme on the hydrophilic surface is also driven by electrostatic attraction as lysozyme is positively charged. Note that the surface consists of carboxyl groups ($pK_a \approx 4.5$) (47) that are negatively charged under the conditions employed here. Analysis of the relationship between frequency change and dissipation change during adsorption of protein reveals that the degree of entrained water in the lysozyme film is similar on both surfaces.

Following protein adsorption and rinsing, SDS is used to affect the removal of protein by exposure to SDS above the CMC for 20 min. Clearly, significant amounts of protein remain (∼32%) on the hydrophilic surface after ten cycles of treatment with SDS, which is much higher than we obtained on the hydrophobic surface. SDS adsorbs strongly, forming a monolayer on the hydrophobic surface through the interaction of the surfactant chain and the surface as well as favorable lateral chain−chain interactions; in contrast, the adsorption of SDS on the negatively charged hydrophilic surface is opposed by the electrostatic repulsion between the headgroup and the surface. Ultimately the hydrophobic surface in the presence of SDS acquires a greater negative charge than the initially negatively charged hydrophilic surface as the carboxyl groups do not fully ionize. We expect the interaction between the SDS and the protein to be largely unchanged; therefore, the relatively low cleaning efficiency of SDS on the hydrophilic surface is attributed to the lower electrostatic repulsion between the negatively charged SDS/protein complex and the negatively charged surface.

In Figure 6, we have investigated the removal of protein from a hydrophilic surface in phosphate buffer by nanobubbles. It can be seen that the frequency change of the lysozyme adsorption is approximately −139 Hz (Sauerbrey mass: ∼ 8.2 mg m^{-2}). Following the same protocol, we present 10 cycles of nanobubble production and removal. It is evident that significant amounts of protein remain (∼32%) on the surface after ten cycles of nanobubble production and removal, and it appears that further cleaning cycles are unable to remove more protein from the surface. This is similar to the result obtained on the hydrophobic surface, indicating that the adsorbed proteins are difficult to remove completely using nanobubbles in phosphate buffer on both hydrophobic and hydrophilic surfaces.

We can conclude that the removal of lysozyme from hydrophilic surfaces is a greater challenge than when hydrophobic surfaces are employed. As we did previously for hydrophobic surfaces, we now investigate if the cleaning efficiency can be improved by using nanobubbles in combination with SDS. In this case, there will be no hydrophobic patches on the surface produced during the cleaning process and hence the sites for nanobubble production should not be directed by spatial variations in wettability.

Figure 7 follows the removal of protein by using the combination of nanobubbles and SDS on a hydrophilic surface. Following the same protocol described above, the SDS/PB solution was replaced by the phosphate buffer after production and removal of nanobubbles. This was followed by exposure to lysozyme (1 mg mL^{-1}) in phosphate buffer. As found previously, the adsorption of lysozyme results in a change of resonance frequency of approximately −132 Hz

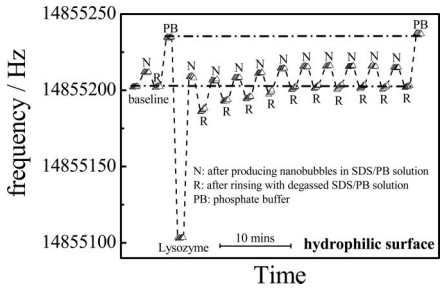

FIGURE 7. Resonance frequency observed for a series of nanobubble production and removal cycles on a hydrophilic surface in SDS/PB solution. The baseline resonance frequency is obtained for a gold-coated crystal bearing a monolayer of 11-mecaptoundecanoic acid in SDS/PB solution. Before lysozyme was introduced, nanobubbles were produced and removed in SDS/PB solution and the SDS/PB solution was replaced by phosphate buffer. N indicates the resonance frequency measured after 10 s of electrochemical treatment to produce nanobubbles and R indicates the resonance frequency measured after the removal of such nanobubbles by rinsing with degassed SDS/PB solution. Subsequently, lysozyme was introduced and the resonance frequency was measured again following a rinse with phosphate buffer. Ten further cycles of nanobubble production and removal in SDS/PB solution are shown. The time scale is indicated by the scale bar.

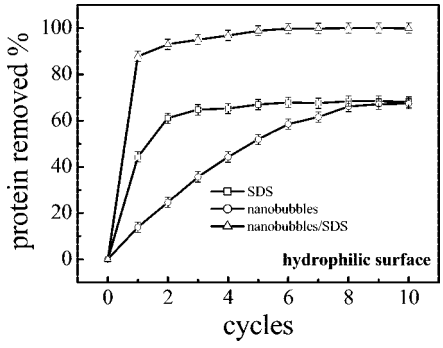

FIGURE 8. Cleaning efficiency obtained using nanobubbles, SDS, or nanobubbles/SDS on a hydrophilic surface. Each cycle is either 10 s of nanobubble production followed by nanobubble removal by means of exchanging the solvent with degassed phosphate buffer (or degassed SDS/PB solution) or 20 min exposure to 17 mM SDS in phosphate buffer followed by rinsing with phosphate buffer (without SDS). The noise level in our frequency measurement is typically less than 1 Hz; however, the main contribution to uncertainty in our measurement is instrumental drift over the time scale of our measurement, which is typically 3 Hz or less. Therefore, the error bars correspond to an error of 3 Hz in our measurements.

and a Sauerbrey mass of ~7.8 mg m^{-2}. Subsequently, 10 cycles of nanobubble production and removal for 10 s periods were conducted. On the very first cycle, a large amount of protein is removed and over subsequent cycles all remaining protein is removed from the surface as evidenced by the resonance frequency of the surface in the rinsed state returning to the baseline frequency.

In Figure 8, we have compared the cleaning efficiencies between nanobubbles, SDS, and nanobubbles in combination with SDS. Clearly, significant amounts of protein remain on the surface after either the 10 cycles of nanobubble treatment or the 10 cycles of SDS treatment in phosphate buffer. The cleaning efficiency of the 20 min treatment with SDS is better than the 10 s treatment with nanobubbles in the first eight cycles, but eventually both of them attain the same cleaning efficiency where 68% protein is removed from the surface. However, the protein can be removed

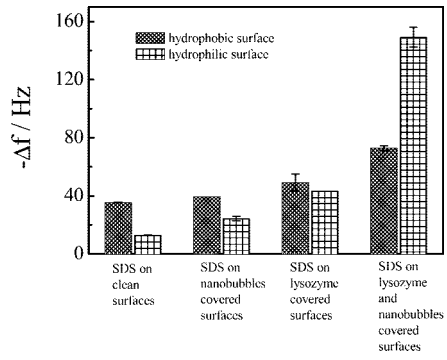

FIGURE 9. Frequency change ($-\Delta f$) induced by the adsorption of SDS on both hydrophobic and hydrophilic surfaces, when the surfaces support different coatings. When protein is present on the surface the values of frequency change reported are obtained from the minima in the frequency versus time plot. This definition was chosen as the adsorption of SDS, which lowers the frequency takes a finite time, but at long times the frequency begins to rise as the protein desorbs from the surface. The error bars come from the repeated experiments.

completely from the surface after only six cycles of treatment when the combination of nanobubbles and SDS is used, indicating strong synergistic effects. We explore these further below.

When SDS is introduced into the system, its adsorption can be followed by the decrease in resonance frequency of the quartz crystal. This is graphically shown in Figure 9 for both hydrophobic and hydrophilic substrates. Note that when protein is present on the surface the values of frequency change ($-\Delta f$) reported are obtained from the minima in the frequency versus time plot. This definition was chosen as the adsorption of SDS, which lowers the frequency takes a finite time, but at long times, the frequency begins to rise as the protein desorbs from the surface.

On the bare surfaces, shown in the first column, very little SDS adsorbs to the hydrophilic surface because of charge repulsion, whereas a surface excess of approximately 2.1 mg m^{-2} (Sauerbrey mass) is obtained on the hydrophobic surface. This adsorption is initially driven by hydrophobic interactions between the SDS chains and the hydrophobic substrate and then by lateral chain−chain interactions forming a monolayer. When a surface with nanobubbles is exposed to SDS greater reductions in resonance frequency are observed, this is shown in the second column. One has to be careful in interpreting these changes in the presence of nanobubbles, as the adsorption of surfactant will change the contact angle and therefore the shape of the nanobubble. It is unclear how this will influence the resonance frequency. Nonetheless, SDS adsorbs readily to the air−water interface and the data are consistent with adsorption at the bubble surfaces and on the exposed substrate, giving a Sauerbrey like response.

When a surface with a coating of lysozyme is exposed to SDS, even greater reductions in resonance frequency are observed and the difference between the hydrophobic and hydrophilic surfaces is small, see the third column. This reflects the high coverage of lysozyme on the surface and the strong interaction between the lysozyme and the SDS. That is, the surface is covered by protein and the underlying

surface is largely not available for adsorption, hence the surfaces are now similar. Thus, this frequency change largely reflects the formation of the SDS/lysozyme complex. The last column in Figure 9 is obtained by adsorbing protein to a surface and then producing nanobubbles on the surface electrochemically for 10 s. The surface in this state is then exposed to SDS and the change in resonance frequency measured. The difference between the hydrophobic and hydrophilic surfaces is dramatic. For the hydrophobic surface, the change in frequency is less than the sum of the values obtained in the second and third column, but greater than each of them individually. This is what might be expected given that the surface is in a sense a combination of the protein covered and nanobubble surfaces and adsorption of SDS to the nanobubble surface will displace protein from the nanobubble surface and in doing so effectively increase the available surface area as the liberated protein will then become available for SDS adsorption.

A very large change in resonance frequency upon exposure is observed for the hydrophilic surface. This far exceeds the sum of the values obtained in the second and third columns. In this case, it is apparent that the presence of nanobubbles enhances the adsorption of SDS to the protein. That is, complexation is greatly enhanced in the presence of nanobubbles. As complexation is an important step in surface cleaning, this enhanced cleaning efficiency can likely be attributed to enhanced complexation. Precisely why nanobubbles result in an enhanced level of complexation is not revealed by our measurements and requires further study.

CONCLUSION

We have investigated the removal of lysozyme from both hydrophobic and hydrophilic surfaces using nanobubbles, SDS, and nanobubbles in combination with SDS using a QCM. On the hydrophobic surface, no obvious improvement in cleaning efficiency of a 10 s treatment with nanobubbles/SDS was obtained over a 20 min treatment with SDS alone. Significant amounts of lysozyme remain on the hydrophilic surface after either 10 cycles of treatment with nanobubbles or 10 cycles of treatment with SDS. In contrast, the protein can be removed completely from a hydrophilic surface after 6 cycles of treatment with nanobubbles in combination with SDS. We attribute this improvement in cleaning efficiency to a synergy between nanobubbles and SDS, which promotes the formation of SDS/lysozyme complexes.

Acknowledgment. V.S.J.C. gratefully acknowledges support from the Australian Research Council.

REFERENCES AND NOTES

(1) Eriksson, J. C.; Ljunggern, S. *Colloids Surf., A* **1999**, *159*, 159.
(2) Ljunggern, S.; Eriksson, J. C. *Colloids Surf., A* **1997**, *129−130*, 151.
(3) Agrawal, A.; Park, J.; Ryu, D.; Hammond, P.; Russell, T.; McKinley, G. *Nano Lett.* **2005**, *5*, 1751.
(4) Holmberg, M.; Kuhle, A.; Garnaes, J.; Morch, K.; Boisen, A. *Langmuir* **2003**, *19*, 10510.
(5) Ishida, N.; Inoue, T.; Miyahara, M.; Higashitani, K. *Langmuir* **2000**, *16*, 6377.
(6) Lou, S. T.; Ouyang, Z. Q.; Zhang, Y.; Li, X. J.; Hu, J.; Li, M. Q.; Yang, F. J. *J. Vac. Sci. Technol., B* **2000**, *18*, 2573.
(7) Switkes, M.; Ruberti, J. W. *Appl. Phys. Lett.* **2004**, *84*, 4759.
(8) Yang, J. W.; Duan, J. M.; Fornasiero, D.; Ralston, J. *J. Phys. Chem. B* **2003**, *107*, 6139.
(9) Fan, Y. W.; Wang, R. Z. *Adv. Mater.* **2005**, *17*, 2384.
(10) Zhang, X. H.; Maeda, N.; Craig, V. S. J. *Langmuir* **2006**, *22*, 5025.
(11) Zhang, X. H.; Khan, A.; Ducker, W. A. *Phys. Rev. Lett.* **2007**, *98*, 136101.
(12) Zhang, X. H.; Zhang, X. D.; Sun, J. L.; Zhang, Z. X.; Li, G.; Fang, H. P.; Xiao, X. D.; Zeng, X. C.; Hu, J. *Langmuir* **2007**, *23*, 1778.
(13) Zhang, L. J.; Zhang, Y.; Zhang, X. H.; Li, Z. X.; Shen, G. X.; Ye, M.; Fan, C. H.; Fang, H. P.; Hu, J. *Langmuir* **2006**, *22*, 8109.
(14) Stöckelhuber, K. W.; Radoev, B.; Wenger, A.; Schulze, H. J. *Langmuir* **2004**, *20*, 164.
(15) Zhang, X. H.; Zhang, X. D.; Lou, S. T.; Zhang, Z. X.; Sun, J. L.; Hu, J. *Langmuir* **2004**, *20*, 3813.
(16) Yang, S.; Dammer, S. M.; Bremond, N.; Zandvliet, H. J. W.; Kooij, E. S.; Lohse, D. *Langmuir* **2007**, *23*, 7072.
(17) Martinez, J.; Stroeve, P. *J. Phys. Chem. B* **2007**, *111*, 14069.
(18) Shen, G.; Zhang, X. H.; Ming, Y.; Zhang, L.; Zhang, Y.; Hu, J. *J. Phys. Chem. B* **2008**, *112*, 4029.
(19) Feng, X.; Roy, S. C.; Grimes, C. A. *Langmuir* **2008**, *24*, 3918.
(20) Zhang, X. H.; Quinn, A.; Ducker, W. A. *Langmuir* **2008**, *24*, 4756.
(21) Jeon, S.; Desikan, R.; Tian, F.; Thundat, T. *Appl. Phys. Lett.* **2006**, *88*, 103118.
(22) Tsionsky, V.; Kaverin, A.; Daikhin, L.; Katz, G.; Gileadi, E. *Phys. Chem. Chem. Phys.* **2005**, *7*, 1830.
(23) Yang, J.; Duan, J.; Fornasiero, D.; Ralston, J. *Phys. Chem. Chem. Phys.* **2007**, *9*, 6327.
(24) Wu, Z. H.; Zhang, X. H.; Zhang, X. D.; Li, G.; Sun, J. L.; Zhang, Y.; Li, M. Q.; Hu, J. *Surf. Interface Anal.* **2006**, *38*, 990.
(25) Wu, Z. H.; Zhang, X. H.; Zhang, X. D.; Sun, J. L.; Dong, Y. M.; Hu, J. *Chin. Sci. Bull.* **2007**, *52*, 1913.
(26) Wu, Z. H.; Chen, H. B.; Dong, Y. M.; Mao, H. L.; Sun, J. L.; Chen, S. F.; Craig, V. S. J.; Hu, J. *J. Colloid Interface Sci.* **2008**, *328*, 10.
(27) Liu, G. M.; Wu, Z. H.; Craig, V. S. J. *J. Phys. Chem. C* **2008**, *112*, 16748.
(28) Sethuraman, A.; Han, M.; Kane, R. S.; Belfort, G. *Langmuir* **2004**, *20*, 7779.
(29) Sarkar, D.; Chattoraj, D. K. *J. Colloid Interface Sci.* **1996**, *178*, 606.
(30) Caruso, F.; Serizawa, T.; Furlong, D. N.; Okahata, Y. *Langmuir* **1995**, *11*, 1546.
(31) Plunkett, M. A.; Claesson, P. M.; Rutland, M. W. *Langmuir* **2002**, *18*, 1274.
(32) Höök, F.; Kasemo, B.; Nylander, T.; Fant, C.; Sott, K.; Elwing, H. *Anal. Chem.* **2001**, *73*, 5796.
(33) Liu, G. M.; Zhao, J. P.; Sun, Q. Y.; Zhang, G. Z. *J. Phys. Chem. B* **2008**, *112*, 3333.
(34) Liu, G. M.; Zou, S. R.; Fu, L.; Zhang, G. Z. *J. Phys. Chem. B* **2008**, *112*, 4167.
(35) Roach, P.; Farrar, D.; Perry, C. C. *J. Am. Chem. Soc.* **2005**, *127*, 8168.
(36) Sauerbrey, G. *Z. Phys.* **1959**, *155*, 206.
(37) Craig, V. S. J.; Plunkett, M. *J. Colloid Interface Sci.* **2003**, *262*, 126.
(38) Kanazawa, K. Z.; Gordon III, J. G. *Anal.Chem.* **1985**, *57*, 1770.
(39) Ferrante, F.; Kipling, A. L.; Thompson, M. *J. Appl. Phys.* **1994**, *76*, 3448.
(40) Ellis, J. S.; Hayward, G. L. *J. Appl. Phys.* **2003**, *94*, 7856.
(41) Du, B. Y.; Goubaidoulline, I.; Johannsmann, D. *Langmuir* **2004**, *20*, 10617.
(42) Su, T. J.; Green, R. J.; Wang, Y.; Murphy, E. F.; Lu, J. R.; Ivkov, R.; Satija, S. K. *Langmuir* **2000**, *16*, 4999.
(43) Tilton, R. D.; Blomberg, E.; Claesson, P. M. *Langmuir* **1993**, *9*, 2102.
(44) Fröberg, J. C.; Blomberg, E.; Claesson, P. M. *Langmuir* **1999**, *15*, 1410.
(45) Green, R. J.; Su, T. J.; Lu, J. R.; Webster, J. R. P. *J. Phys. Chem. B* **2001**, *105*, 9331.
(46) Arai, T.; Norde, W. *Colloids Surf.* **1990**, *51*, 1.
(47) Gebhardt, J. E.; Fuerstenau, D. W. *Colloids Surf.* **1983**, *7*, 221.

AM800150P